Published in "Blood doi: 10.1182/blood-2013-01-479311, 2013"
which should be cited to refer to this work.

Virus-associated activation of innate immunity induces rapid disruption of Peyer's patches in mice

Simon Heidegger[1,*], David Anz[1,*], Nicolas Stephan[1], Bernadette Bohn[1], Tina Herbst[2], Wolfgang Peter Fendler[1], Nina Suhartha[1,2], Nadja Sandholzer[1], Sebastian Kobold[1], Christian Hotz[1,2], Katharina Eisenächer[3], Susanne Radtke-Schuller[4], Stefan Endres[1], Carole Bourquin[1,2]

[1]Center for Integrated Protein Science Munich (CIPSM), Division of Clinical Pharmacology, Medizinische Klinik und Poliklinik IV, Ludwig-Maximilians-Universität München, 80336 Munich, Germany
[2]Chair of Pharmacology, Department of Medicine, Faculty of Science, University of Fribourg, 1700 Fribourg, Switzerland
[3]II. Medizinische Klinik, Klinikum Rechts der Isar, Technische Universität München, 81675 Munich, Germany
[4]Dpt. Biology II, Ludwig-Maximilians-Universität München, 82152 Planegg-Martinsried, Germany.

*These authors contributed equally.

Corresponding Author: Carole Bourquin, University of Fribourg, 1700 Fribourg, Switzerland
Phone: 0041 26 300 9411; Fax: 0041 26 300 9683; Email: carole.bourquin@unifr.ch

Running title: Virus-associated disruption of Peyer's patches

Scientific category: Immunobiology

ABSTRACT

Key Points:

1. Systemic virus infection leads to rapid disruption of the Peyer's patches but not of peripheral lymph nodes.
2. Virus-associated innate immune activation and type I interferon release blocks trafficking of B cells to Peyer's patches.

Early in the course of infection, detection of pathogen-associated molecular patterns by innate immune receptors can shape the subsequent adaptive immune response. Here we investigate the influence of virus-associated innate immune activation on lymphocyte distribution in secondary lymphoid organs. We show for the first time that virus infection of mice induces rapid disruption of the Peyer's patches but not of other secondary lymphoid organs. The observed effect was not dependent on an active infectious process but due to innate immune activation and could be mimicked by virus-associated molecular patterns such as the synthetic double-stranded RNA poly(I:C). Profound histomorphological changes in Peyer's patches were associated with depletion of organ cellularity, most prominent among the B cell subset. We demonstrate that the disruption is entirely dependent on type I interferon. At the cellular level, we show that virus-associated immune activation by IFN-α blocks B-cell trafficking to the Peyer's patches by downregulating expression of the homing molecule $\alpha_4\beta_7$-integrin. In summary, our data identify a mechanism that results in type I IFN-dependent rapid but reversible disruption of intestinal lymphoid organs during systemic viral immune activation. We propose that such re-routed lymphocyte trafficking may impact the development of B cell immunity to systemic viral pathogens.

INTRODUCTION

The innate immune system represents the first line of defense against invading viruses. The initiation of an anti-viral response is critically dependent on the detection of specific pathogen-associated molecular patterns by innate immune pattern-recognition receptors.[1] These patterns are evolutionarily highly conserved molecular structures shared by a variety of different viruses. One such pattern is viral RNA, which can be detected by members of the retinoic acid inducible gene I (RIG-I)-like receptor and Toll-like receptor (TLR) families.[2,3] Activation of these receptors leads to the initiation of an innate immune response characterized by the rapid production of pro-inflammatory cytokines such as the type I interferons (IFN) IFN-α and IFN-β. At the infected site, type I IFNs act in concert with other cytokines to hinder the replication and spread of virus and to recruit inflammatory cells. In addition, these cytokines have systemic effects that can critically shape the subsequent adaptive immune response.[4]

Adaptive immunity depends on lymphocyte maturation in primary lymphoid organs, their tightly regulated release into the circulation and accurate positioning in secondary lymphoid organs. Several reports have recently highlighted the impact of virus-associated type I IFNs on lymphocyte development and distribution: In bone marrow, dormant hematopoietic stem cells that give rise to virtually all leukocytes have been shown to enter the cell cycle after intravenous injection of type I IFNs and during virus infection.[5] We and others have demonstrated that activation of virus-sensing innate immune receptors with the synthetic double-stranded RNA poly(I:C) leads to type I IFN-dependent rapid involution of the thymus. [6] In skin-draining peripheral lymph nodes (PLN), poly(I:C)-induced type I IFNs have been shown to block lymphocyte egress which results in temporary lymphoid organ 'shutdown'.[7] However, little is known about the influence of virus infection on lymphocyte distribution in secondary lymphoid organs of the intestinal immune compartment.

Many viruses, including those classically considered non-enteric, frequently show intestinal involvement, either due to direct infection of the gut mucosa or to collateral effects.[8] In the course of such an enteric infection, aggregated lymphoid follicles in the gut wall - the Peyer's patches - form the primary inductive site of intestinal anti-microbial immunity.[9,10] In this study, we investigated the effect of virus-associated innate immune activation on lymphocyte distribution within these organs. Here we show for the first time that viral immune activation substantially changes the morphology of the Peyer's patches by inducing their rapid disruption. A marked type I IFN-dependent loss of cellularity was associated with strongly reduced B cell trafficking to the Peyer's patches. Our data identify a mechanism that results in rapid but reversible loss of B cells in Peyer's patches during virus-associated systemic

innate immune activation. We hypothesize that such re-routing of lymphocyte trafficking during systemic infection may be important for effective anti-viral B cell immunity.

METHODS

Mice. Female C57BL/6 mice were purchased from Harlan-Winkelmann and Janvier. Type I IFN receptor-deficient mice ($IFNaR^{-/-}$) were backcrossed 20 times on the C57BL/6 background [11]. Mice were at least 8 weeks of age at the onset of experiments. All animal studies were approved by the local regulatory agency (Regierung von Oberbayern, Munich, Germany).

Injection of poly(I:C), recombinant IFN-α, virus and blocking antibody. Mice were injected i.p. with poly(I:C) (InvivoGen) (250 µg in PBS). For examination of lymphoid organ cellularity, mice were treated twice at a 3-day interval. In all other experiments, mice were treated with a single injection of poly(I:C). Where indicated, mice were provided with drinking water supplemented with FTY720 (Sigma, 2 µg/ml) beginning two days prior to the first poly(I:C) treatment. IFN-α (Miltenyi) was applied i.p. (12 µg in 200 µl PBS) daily on 6 consecutive days. 24 h after the last injection, lymphoid organs were examined. For viral infection, mice were i.p. injected with 10^6 pfu of VSV *Indiana strain* in 200 µl PBS. Lymphoid organs were examined 2 or 5 days after virus injection. For *in vivo*-$\alpha_4\beta_7$-blockade, mice were injected i.p. with 75 µg anti-$\alpha_4\beta_7$ antibody (clone DATK32) or a rat IgG2a control antibody (AbD Serotec, Puchheim, Germany) in 100 µl PBS. Purification of DATK32 antibody from the DATK32 hybridoma cell line (ATCC, Manassas, USA) is described in detail in the Supplementary Material and Methods.

Tissue preparation. Tissue single cell suspensions were prepared as described previously.[12] For the determination of lymphocyte numbers in secondary lymphoid organs, bilateral inguinal and axillary lymph nodes were pooled (PLNs). For mesenteric lymph nodes, all lymph nodes along the full length of the superior mesenteric artery to the aortic root were dissected as described.[13] All Peyer's patches were prepared and were pooled for further analysis. Isolation of lymphocytes from small intestine lamina propria was performed as described previously.[14] Briefly, small intestine was removed 0.5 cm below stomach and 1 cm above cecum. Peyer's patches were removed surgically. The intestine was opened longitudinally and cut into pieces of 0.5-1 cm in length. Epithelial cells and intraepithelial lymphocytes were detached by several washing steps with HBSS containing 1 mM DTT or 1.3 mM EDTA. Pieces of small intestine were then enzymatically digested with the help of collagenase VIII (Sigma). Single cell suspensions were purified using 44%-67% percoll (Sigma) gradient centrifugation.

Flow cytometry. Antibodies to CD3 (Clone: 17A2), CD4 (RM4-5), CD8 (53-6.7), CD11c (N418), CD19 (6D5), CD69 (H1.2F3), $\alpha_4\beta_7$ (DATK32) and CD62L (MEL-14) were purchased

from BioLegend. Antibodies to Foxp3 (FJK-16a) and $S1P_1$ (713412) were from Ebioscience and R&D Systems. Cells were stained in PBS supplemented with 10% FCS and were analyzed using a FACSCanto II (BD Biosciences). For intracellular staining, single-cell suspensions were fixed and permeabilized using a ready-mixed kit from Ebioscience. Fluorescence associated with non-specific binding was subtracted using subtype-specific isotype controls. All data were evaluated with FlowJo software (Treestar).

Histology and immunohistochemistry. For regular histology specimens were fixed in formalin before embedding in paraffin blocks. Tissue sections were stained with Hematoxylin and Eosin (H&E). Images were obtained using light microscopy. For immunohistochemistry tissue was deep-frozen in OCT and cryosections of 5 µm were prepared and fixed with ice-cold acetone. Sections were rehydrated with PBS and blocking was performed using 10 % goat-serum in PBS. For fluorescent labeling unconjugated anti-B220 (RA3-6B2, Biolegend) primary antibody, followed by anti-rat IgG Cy3-conjugated antibody (112-165-1430, Jackson ImmunoResearch) and DAPI (Biotium) for counterstaining were used. Pictures were taken with a standard fluorescent microscope and processed with Adobe Photoshop to adjust size.

Cell purification and adhesion assay. B cells from different secondary lymphoid organs were enriched using a MACS $CD19^+$ B cell isolation kit according to the manufacturer's protocol (Miltenyi Biotech). Purity of magnetically sorted B cells was > 95 %. 96-well plates were coated with recombinant mouse MAdCAM-Fc chimera (10 µg/ml, R&D Systems) overnight at 4 °C. The supernatant was then discarded and wells blocked with 1 % BSA in PBS for 3 h at room temperature. Purified B cells were cultured in RPMI 1640 medium supplemented with 10% FCS, 2 mM L-glutamine, 100 µg/mL streptomycin, and 1 IU/mL penicillin (complete RPMI) in the presence of recombinant IFN-α ($1x10^3$ U/ml). B cells were labeled with CFSE (Invitrogen) according the manufacturer's protocol. Cells (10^7/ml in DMEM without phenol red supplemented with 25 mM HEPES) were pre-incubated in polypropylene tubes with or without DATK32, MEL-14 or M17/4 antibody (10 µg/ml, all from BioLegend) for 25 min at 37 °C before cells were added to coated plates and incubated for 35 min at 37 °C and 5 % CO_2. Non-adherent cells were removed by 2 to 3 washing steps with PBS. Fluorescent emission of adhesive cells was measured with a plate reader.

***In vivo* homing experiments.** Splenic B cells were cultured in complete RPMI with or without added IFN-α ($1x10^3$ U/ml) for 24 h. Subsequently, the two cell cultures were stained with CFSE or Cell Tracker violet (both 5 µM, Molecular Probes) according to the manufacturer's protocol. 1 x 10^7 cells from each preparation were mixed and injected i.v. into naïve recipient mice. An aliquot was saved to assess the input ratio. 6 hours after the

adoptive transfer, cell preparations from different recipient tissues were analyzed for adoptively transferred B cells by flow cytometry. The homing index (HI) was calculated as the ratio of $[\text{IFN-}\alpha\text{ B cells}]_{tissue}$ / $[\text{untreated B cell}]_{tissue}$ to $[\text{IFN-}\alpha\text{ B cells}]_{input}$ / $[\text{untreated B cell}]_{input}$ as described previously.[15]

Serum IgA levels. For the analysis of total serum immunoglobulin (Ig) G and IgA levels, 96-well plates (Nunc) were coated with goat anti-mouse IgA or goat anti-mouse IgG (Southern Biotech). For detection peroxidase-linked anti-mouse alpha-chain or gamma-chain specific secondary antibody (Sigma) and TMB substrate kit (BD Bioscience) were used.

Statistics. All data are presented as mean ± S.E.M. Statistical significance of single experimental findings was assessed with the independent two-tailed Student's t-test. For multiple statistical comparison of a data set the one-way ANOVA test with Bonferroni post-test was used. Significance was set at *P* values < 0.05, $p < 0.01$ and $p < 0.001$ and was then indicated with an asterisk (*, ** and ***). All statistical calculations were performed using Graphpad Prism (GraphPad Software).

RESULTS

Virus-associated immune activation causes rapid disruption of Peyer's patches.

To examine the effect of virus infection on the distribution of lymphocytes in intestinal lymphoid organs, we injected mice intraperitoneally with the negative strand RNA virus vesicular stomatitis virus (VSV). This model is characterized by rapid viral spread to multiple body compartments and high systemic levels of type I IFN induction.[16] On inspection of the small intestine, the Peyer's patches of VSV-infected mice showed pronounced reduction in organ size that was due to a loss in cellularity **(Fig. 1A)**. A similar disruption was observed when mice were treated with poly(I:C), a synthetic double-stranded RNA analog. Poly(I:C) mimics a viral molecular pattern and stimulates the innate immune system through the activation of the Toll-like receptor 3 and the family of RIG-like helicases.[2,3] Adult mice were injected twice intraperitoneally with poly(I:C) at a 3-day interval and organs were examined 48 h after the second injection. The total number of Peyer's patches was markedly reduced in poly(I:C)-treated mice and the remaining Peyer's patches were macroscopically barely visible. On average, less than two Peyer's patches were identified in poly(I:C)-treated vs. eight Peyer's patches or more in untreated mice **(Fig. 1B)**. The cell numbers in Peyer's patches dropped by more than 70 %. In contrast, in mesenteric lymph nodes or skin-draining PLN cellularity remained unchanged after poly(I:C) treatment **(Fig. 1C)**. Morphologically, the Peyer's patches are formed by aggregated lymphoid follicles surrounded by the corona or subepithelial dome.[17] To assess changes in Peyer's patch microanatomy, organs from poly(I:C)-treated mice were examined histologically. The sections showed striking changes in the Peyer's patch architecture: Lymphoid follicles were barely visible and the width of the subendothelial dome was markedly reduced **(Fig. 1D).** This effect was independent of the injection route of poly(I:C) as the disruption of the Peyer's patches did not differ when poly(I:C) was applied intravenously instead of intraperitoneally **(Fig. S1)**.

In the remaining Peyer's patches, the poly(I:C)-induced loss of cellularity affected all lymphocyte subsets **(Fig. 2A)**. However, the effect was most prominent among B cells which form the most abundant lymphocyte population in these lymphoid organs.[17] Indeed, the overall frequency of B cells within the Peyer's patches dropped by 37 $\pm$ 14 % whereas other cell types showed constant frequencies **(Fig. 2B)**. In contrast, in PLN the absolute number and frequency of B cells were increased following poly(I:C) treatment **(Fig. 2C+D)**. Because the observed loss of cellularity was mainly due to decreased B cell numbers, we focused our following work on this subset.

Disruption of the Peyer's patches is dependent on type I interferons.

In the mammalian anti-viral immune response, the release of type I interferon plays a central role. Activation of pattern-recognition receptors by poly(I:C) leads to the production of a large amount of the type I interferons IFN-α and IFN-β which both signal through the IFN-α receptor (IFNaR).[18] To investigate the role of type I IFN in poly(I:C)-induced disruption of the Peyer's patches, we treated IFNaR-deficient mice ($IFNaR^{-/-}$) with poly(I:C). In contrast to the reduced cellularity in Peyer's patches of wild-type mice, $IFNaR^{-/-}$ mice showed no change in cell numbers in these organs following poly(I:C) treatment **(Fig. 3A)**. Furthermore, treatment of mice with recombinant IFN-α also led to the disruption of Peyer's patches, demonstrating a direct involvement of type I IFN **(Fig. 3B)**. Two essential mechanisms by which type I IFN can prevent viral replication are the induction of apoptosis[19] and the suppression of proliferation in host cells.[20] To investigate whether these mechanisms were involved in the disruption of Peyer's patches, we first quantified B cell proliferation by measuring their *in vivo* incorporation of BrdU. Following poly(I:C) treatment, we observed an increased B cell proliferation in the spleen but no changes within Peyer's patches or PLN **(Fig. S2A)**. To evaluate the role of apoptosis in the disruption of Peyer's patches, we determined the percentage of apoptotic B cells within lymphoid organs upon treatment with poly(I:C). Surprisingly, early apoptotic B cells were slightly reduced in both PLN and Peyer's patches whereas there was little increase in late apoptotic B cells in Peyer's patches **(Fig. S2B)**. Taken together, these data show that the disruption of the Peyer's patches following poly(I:C) treatment is dependent on type I IFN but cannot be explained by changes in B cell proliferation or apoptosis.

Treatment of mice with the $S1P_1$-blocking agent FTY720 counteracts immune-induced disruption of the Peyer's patches.

Previous reports have demonstrated that the sphingosine-1 phosphate receptor 1 ($S1P_1$) is essential for lymphocyte recirculation and that it regulates egress from both thymus and peripheral lymphoid organs.[21] Following poly(I:C) treatment, type I IFN has been shown to induce lymphocyte expression of CD69 which forms a complex with and thus negatively regulates $S1P_1$, resulting in reduced T and B cell efflux from PLN and their accumulation in these lymph nodes.[7] Based on our novel findings that organ cellularity increases in PLN but decreases in Peyer's patches following innate immune activation, we hypothesized that $S1P_1$-dependent B cell efflux from these tissues might be regulated in opposite ways. Thus, the poly(I:C)-induced disruption of Peyer's patches could be caused by an enhanced B cell egress from these organs. To investigate whether B cell efflux from Peyer's patches is increased during innate immune activation, mice were injected twice with poly(I:C) following pretreatment with FTY720. This immunosuppressant drug has been shown to inhibit

lymphocyte emigration from lymphoid organs by downregulating $S1P_1$.[21] FTY720 treatment alone did not significantly change absolute cell numbers in Peyer's patches or PLN **(Fig. 4)**. Strikingly, mice that were pretreated with FTY720 did not show reduced cellularity of Peyer's patches following two injections of poly(I:C). Thus, FTY720 treatment counteracts the poly(I:C)-induced disruption of Peyer's patches. In view of the known effect of FTY720 on $S1P_1$-mediated lymphocyte migration, we concluded that the disruption might be due to increased $S1P_1$-dependent lymphocyte egress.

Stimulation with type I interferon results in reduced B cell homing to Peyer's patches.

To test this hypothesis, we compared $S1P_1$ mRNA levels in B cells from PLN and Peyer's patches following poly(I:C) treatment. In line with with previous reports,[7] $S1P_1$ transcripts were rapidly reduced in B cells from PLN **(Fig. S3A)**. However, B cells in Peyer's patches also showed downregulated $S1P_1$ mRNA levels after poly(I:C) treatment. Flow cytometry analysis confirmed that B cells in both PLN and Peyer's patches showed similarly reduced expression of $S1P_1$ after injection of poly(I:C) **(Fig. S3B).** As described previously[21], the reduced expression of $S1P_1$ on B cells from PLN of poly(I:C)-treated mice translated into impaired B cell ability to migrate towards a S1P gradient *in vitro* **(Fig. S3C).** B cells prepared from Peyer's patches of poly(I:C)-treated mice showed similarly reduced *in vitro*-chemotaxis towards S1P. Taken together, these data demonstrate that following poly(I:C) treatment, B cells in Peyer's patches do not show an increase but rather a decrease in $S1P_1$-dependent migration, similar to the reduced migration described for B cells in PLN.[21] Hence, the striking difference in cellularity of Peyer's patches and PLN in poly(I:C)-treated mice is unlikely to be due to opposite regulation of $S1P_1$-dependent lymphocyte egress.

Previous reports highlighted that FTY720 not only affects $S1P_1$-dependent egress of lymphocytes but also enhances their homing into secondary lymphoid organs.[22] We therefore hypothesized that poly(I:C) and type I interferon cause disruption of Peyer's patches by decreasing the entry of B cells into these organs and that this mechanism is counteracted by FTY720. Lymphocyte homing is guided by a pattern of site-specific surface molecules such as integrins that direct them to different tissue compartments. The integrin $\alpha_4\beta_7$ is essential for lymphocyte entry into Peyer's patches and the intestinal lamina propria through interaction with its ligand, the mucosal addressin cell adhesion molecule-1 (MAdCAM-1), which is locally expressed on specialized high endothelial venules in these tissues.[23-25] At the same time lymphocytes express CD62L (L-Selectin) which allows for their influx into PLN[26] but also plays a role in their migration to Peyer's patches.[27] To investigate whether type I IFN-dependent disruption of Peyer's patches might be due to reduced B cell entry into these lymphoid organs, we first determined the expression of the adhesion molecules $\alpha_4\beta_7$ and

CD62L on IFN-α-treated splenic B cells. IFN-α-activated B cells showed increased expression of the early activation marker CD69 and moderately increased levels of CD62L but downregulated surface expression of the gut-homing integrin $\alpha_4\beta_7$ **(Fig. 5A)**. Consistent with these findings, IFN-α-stimulated B cells showed reduced *in vitro*-binding to MAdCAM-1 **(Fig. 5B)**. This reduction was comparable to that seen with an $\alpha_4\beta_7$-blocking antibody. Pretreatment with antibodies that inhibit the adhesion molecules CD62L or LFA-1 did not influence B cell adhesion to recombinant MAdCAM-1.

The modified expression pattern of adhesion molecules and binding characteristics of the IFN-α-activated B cells translated into an essentially altered *in vivo* homing behavior. Following adoptive transfer into naïve recipient mice, IFN-α-activated B cells showed reduced immigration into Peyer's patches when compared to co-transferred unstimulated cells **(Fig. 5C)**. In contrast, IFN-α pretreatment increased B cell migration to PLN. Homing to spleen was not influenced by IFN-α activation. Taken together, these data demonstrate that IFN-α downregulates expression of the gut-homing molecule $\alpha_4\beta_7$ and selectively blocks B-cell trafficking to the Peyer's patches. Thus, we conclude that poly(I:C) and type I interferon-induced disruption of the Peyer's patches is caused by a reduced influx of B cells into the Peyer's patches. Indeed, acute blockade of $\alpha_4\beta_7$ function *in vivo* following a single injection of anti-$\alpha_4\beta_7$ antibody led to rapid loss of Peyer's patch cellularity **(Fig. 5D)**, whereas cell numbers in spleen and peripheral lymph nodes were not significantly altered. Thus, the changes in organ cellularity induced by $\alpha_4\beta_7$ blockade mirror the effects of poly(I:C)-mediated type I IFN release.

Previous reports have demonstrated that expression of the $\alpha_4\beta_7$ integrin is not only important for B-cell entry into Peyer's patches but also for their trafficking to the intestinal lamina propria; this being a prerequisite for the effective clearance of an intestinal virus infection.[28] Therefore, we investigated whether downregulation of $\alpha_4\beta_7$ following virus-associated innate immune activation has an impact on lymphocyte distribution in the intestinal lamina propria. Repetitive treatments with poly(I:C) did not influence lymphocyte numbers nor their localization within the small intestine lamina propria **(Fig. 6A,B).** Compatibly, serum levels of IgA, that is predominantly associated with mucosal immunity, were not altered following poly(I:C) treatment **(Fig. 6C)**.

Disruption of the Peyer's patches is a self-limiting process.

Upon viral infection or stimulation by synthetic ligands such as poly(I:C), the secretion of type I IFN is typically an early and short-lasting event.[29] As the Peyer's patch loss in cellularity is dependent on type I interferons, we examined whether the effect is reversible upon

termination of IFN-inducing poly(I:C) treatment. Therefore, we examined $\alpha_4\beta_7$ and CD69 expression following a single injection of poly(I:C) on circulating B cells which give rise to the Peyer's patches B cell population. And indeed the downregulation of the gut-homing integrin $\alpha_4\beta_7$ observed on B cells after poly(I:C) treatment peaked around 12 h and was restored to baseline level 96 h post injection **(Fig. 7A, B)**. Interestingly, this process occured simultaneously with the upregulation of the activation marker CD69 which has been shown to bind and negatively regulate $S1P_1$.[7] In line with the transient $\alpha_4\beta_7$ downregulation, diminished cellularity of the Peyer's patches induced by two consecutive poly(I:C) treatments had returned to baseline levels 20 days after the last injection **(Fig. 7C)**. These data suggest that immune-induced disruption of Peyer's patches is self-limiting and that organ integrity is restored after cessation of viral innate immune activation.

DISCUSSION

The disruption of Peyer's patches observed in our study is reminiscent of the changes described in mice that genetically lack the adhesion molecule β_7 integrin or its regulating transcription factor, Kruppel-like factor 2.[30,31] These mice are characterized by smaller numbers of Peyer's patches and reduced cellularity within these organs compared to wild-type mice. Furthermore, we show a similar phenotype after a single injection of a neutralizing antibody against $\alpha_4\beta_7$ resulting in a rapid and strong decrease in the cellularity of Peyer's patches. In transfer experiments, we have shown that IFN-α stimulation selectively impairs migration of B cells to Peyer's patches, whereas recirculation to PLNs is moderately increased. This homing pattern mimics the migratory capacity of lymphocytes that either genetically lack the β_7 subunit or have been treated with neutralizing antibodies against the $\alpha_4\beta_7$ heterodimer or its subunits.[24,30,32] Indeed, we demonstrate that IFN-α-activated B cells downregulate the integrin heterodimer $\alpha_4\beta_7$ and that this is associated with reduced binding to its endothelial ligand MAdCAM-1. In contrast to the impaired homing to the Peyer's patches, β_7-deficient lymphocytes have been described to show only little change in recirculation to mesenteric or peripheral lymph nodes. This is due to the redundant activity of the adhesion molecule CD62L, which can partly compensate for the absence of $\alpha_4\beta_7$.[33] Compatibly, we observed a moderately increased expression of CD62L following virus-associated innate immune activation and stable B cell numbers in mesenteric and peripheral lymph nodes. We also observed that B cell distribution within the intestinal lamina propria, which is also dependent on the $\alpha_4\beta_7$ integrin, was not altered following virus-associated innate immune activation. In general, the changes in B-cell trafficking to GALT following viral immune activation show parallels to the recently observed modifications in the homing of bystander-activated CD8 T cells during acute bacterial infection. [34]

Disruption of the Peyer's patches was prevented when mice were pretreated with the immunomodulatory compound FTY720, which was initially described to block $S1P_1$-dependent lymphocyte egress from thymus and peripheral lymph nodes.[21] However, after poly(I:C) immune activation we did not observe increased B cell responsiveness to S1P in Peyer's patches, which could have accounted for reduced organ cellularity and disruption. Thus, the prevention of Peyer's patch disruption associated with FTY720 was unlikely to stem from a blockage of B cell egress from secondary lymphoid organs. Indeed, a later study suggested that, in addition to its effect on lymphocyte egress, FTY720 can reinforce lymphocyte interactions with high endothelial venules and thus rescue the immigration defects of β_2 or β_7 integrin single-deficient lymphocytes into secondary lymphoid organs.[35] Thereby, FTY720 treatment does not activate alternative homing mechanisms but rather

seems to shift the balance of distinct molecular mechanisms during the extravasation process by extending the retention time of the lymphocytes on the endothelial surfaces. We suggest that the absence of Peyer's patches disruption in FTY720-pre-treated mice is due to reinforced lymphocyte-endothelium interactions that compensate for reduced B cell $\alpha_4\beta_7$ expression upon poly(I:C) injection. In line with previous reports,[21] we found that administration of FTY720 led to pronounced lymphopenia, which is however not expected to significantly impact homeostatic lymphocyte homing to the Peyer's patches.[36]

Interestingly, we found that reduced B cell expression of $\alpha_4\beta_7$ and associated disruption of Peyer's patches is self-limiting and that lymphoid organ cell numbers return to baseline levels once the systemic immune activation induced by virus-associated molecular patterns has ceased. Such transient modulation of factors that influence homeostatic trafficking and motility of lymphocytes has been suggested as a mechanism of the adaptive immune response to orchestrate local cellularity, thus limiting competition for space and resources during ongoing immune responses.[37] Indeed, Mueller et al. demonstrated that during viral infection certain chemokines which guide lymphocyte migration into lymphoid organs can be downregulated, thereby shaping the specificity of the newly generated memory cell pool. Our findings show two new aspects of this concept: a) that not only chemokines but also integrins participate in these regulatory mechanisms and b) trafficking of newly activated non-cognate lymphocytes can be controlled in a tissue-specific manner.

During systemic infection, the type I IFN-dependent transient re-routing of B cell trafficking may also serve to redirect a polyclonal population of B cells to the systemic circulation where antigens are present. Indeed, systemic infection of mice with murine leukaemia viruses leads to a dramatic enlargement of spleen and lymph nodes that is associated with atrophy of the Peyer's patches and a predominant B cell loss.[38] Oral infection with rotavirus, a pathogen with gastrointestinal tropism, leads to hyperplasia of the Peyer's patches in mice[10,39]. In this model of intestinal infection, local proliferation of antigen-specific B and T cells in the Peyer's patches may block or simply mask reduction in non-cognate B cells.[28,40] During chronic virus infections, prolonged type I IFN release has been associated with hyperimmune activation, disruption of lymphoid tissue architecture and disease progression.[41,42] It is thus possible that during chronic immune activation, prolonged changes in B cell homing patterns may in fact hinder the control of virus replication. Generally, understanding the regulation of lymphocyte distribution during viral immune activation may open new possibilities for the treatment of associated immune pathologies. In addition, potent synthetic inducers of type I IFN such as poly(I:C) have evolved as a promising tool to modulate the immune system for therapeutic purposes [43]. Recombinant type I interferons are commonly used for the treatment of cancer

and chronic viral infections such as hepatitis.[44,45] Such therapeutic utilization of highly-concentrated type I IFN could affect Peyer's patch cellularity in humans and thus their impact on intestinal immune function should be considered, especially in the case of chronic regimens.

ACKNOWLEDGMENTS

We thank G. Ziegleder (University Munich) for help with histology sections. This work was supported by grants from the LMUexcellent research professorship (to S.E.), the German Research Foundation: DFG En 169/7-2 and Graduiertenkolleg 1202 (to C.B., S.E. and S.H.), the Swiss National Science Foundation (project 138284 to C.B.), Krebsforschung Schweiz (KFS 2910-02-2012), the excellence cluster Center for Integrated Protein Science Munich 114 (to S.E.), and BayImmuNet (to C.B., S.K. and S.E.). This work is part of the doctoral theses of B.B., N.St. and N.Su. at the Ludwig-Maximilian University of Munich.

AUTHORSHIP CONTRIBUTIONS

S.H., D.A. and C.B. designed the research, analyzed and interpreted the results, S.H. and C.B. prepared the manuscript. S.H., B.B., N.St., WP.F., N.Su., N.Sa. and T.H. did the experiments. S.R-S. did histology sections. K.E. performed virus infections. C.H. and S.K. gave methodological support and conceptual advice. C.B. and S.E. guided the study.

The authors declare no financial conflicts of interest.

REFERENCES

1. Kato H, Takahasi K, Fujita T. RIG-I-like receptors: cytoplasmic sensors for non-self RNA. *Immunol Rev*. 2011;243(1):91-98.
2. Kato H, Takeuchi O, Sato S, et al. Differential roles of MDA5 and RIG-I helicases in the recognition of RNA viruses. *Nature*. 2006;441(7089):101-105.
3. Barton GM. Viral recognition by Toll-like receptors. *Semin Immunol*. 2007;19(1):33-40.
4. Lopez CB, Hermesh T. Systemic responses during local viral infections: type I IFNs sound the alarm. *Curr Opin Immunol*. 2011;23(4):495-499.
5. Essers MA, Offner S, Blanco-Bose WE, et al. IFNalpha activates dormant haematopoietic stem cells in vivo. *Nature*. 2009;458(7240):904-908.
6. Anz D, Thaler R, Stephan N, et al. Activation of melanoma differentiation-associated gene 5 causes rapid involution of the thymus. *J Immunol*. 2009;182(10):6044-6050.
7. Shiow LR, Rosen DB, Brdicková N, et al. CD69 acts downstream of interferon-alpha/beta to inhibit S1P1 and lymphocyte egress from lymphoid organs. *Nature*. 2006;440(7083):540-544.
8. Openshaw PJ. Crossing barriers: infections of the lung and the gut. *Mucosal Immunol*. 2009;2(2):100-102.
9. Narvaez CF, Angel J, Franco MA. Interaction of rotavirus with human myeloid dendritic cells. *J Virol*. 2005;79(23):14526-14535.
10. Lopez-Guerrero DV, Meza-Perez S, Ramirez-Pliego O, et al. Rotavirus infection activates dendritic cells from Peyer's patches in adult mice. *J Virol*. 2010;84(4):1856-1866.
11. Muller U, Steinhoff U, Reis LF, et al. Functional role of type I and type II interferons in antiviral defense. *Science*. 1994;264(5167):1918-1921.
12. Bourquin C, Schmidt L, Hornung V, et al. Immunostimulatory RNA oligonucleotides trigger an antigen-specific cytotoxic T-cell and IgG2a response. *Blood*. 2007;109(7):2953-2960.
13. Macpherson AJ, Uhr T. Induction of protective IgA by intestinal dendritic cells carrying commensal bacteria. *Science*. 2004;303(5664):1662-1665.
14. Sheridan BS, Lefrancois L. Isolation of mouse lymphocytes from small intestine tissues. *Curr Protoc Immunol*. 2012;Chapter 3:Unit3 19.
15. Mora JR, Bono MR, Manjunath N, et al. Selective imprinting of gut-homing T cells by Peyer's patch dendritic cells. *Nature*. 2003;424(6944):88-93.
16. Trottier MD, Lyles DS, Reiss CS. Peripheral, but not central nervous system, type I interferon expression in mice in response to intranasal vesicular stomatitis virus infection. *J Neurovirol*. 2007;13(5):433-445.

17. Jung C, Hugot JP, Barreau F. Peyer's Patches: The Immune Sensors of the Intestine. *Int J Inflam*. 2010;2010:823710.

18. Uze G, Schreiber G, Piehler J, Pellegrini S. The receptor of the type I interferon family. *Curr Top Microbiol Immunol*. 2007;316:71-95.

19. Clemens MJ. Interferons and apoptosis. *J Interferon Cytokine Res*. 2003;23(6):277-292.

20. Petricoin EF, 3rd, Ito S, Williams BL, et al. Antiproliferative action of interferon-alpha requires components of T-cell-receptor signalling. *Nature*. 1997;390(6660):629-632.

21. Matloubian M, Lo CG, Cinamon G, et al. Lymphocyte egress from thymus and peripheral lymphoid organs is dependent on S1P receptor 1. *Nature*. 2004;427:355-360.

22. Henning G, Ohl L, Junt T, et al. CC chemokine receptor 7-dependent and -independent pathways for lymphocyte homing: modulation by FTY720. *J Exp Med*. 2001;194(12):1875-1881.

23. Bargatze RF, Jutila MA, Butcher EC. Distinct roles of L-selectin and integrins alpha 4 beta 7 and LFA-1 in lymphocyte homing to Peyer's patch-HEV in situ: the multistep model confirmed and refined. *Immunity*. 1995;3(1):99-108.

24. Wagner N, Lohler J, Kunkel EJ, et al. Critical role for beta7 integrins in formation of the gut-associated lymphoid tissue. *Nature*. 1996;382(6589):366-370.

25. Agace WW. Tissue-tropic effector T cells: generation and targeting opportunities. *Nat Rev Immunol*. 2006;6(9):682-692.

26. Arbones ML, Ord DC, Ley K, et al. Lymphocyte homing and leukocyte rolling and migration are impaired in L-selectin-deficient mice. *Immunity*. 1994;1(4):247-260.

27. von Andrian UH, Mackay CR. T-cell function and migration. Two sides of the same coin. *N Engl J Med*. 2000;343(14):1020-1034.

28. Williams MB, Rose JR, Rott LS, Franco MA, Greenberg HB, Butcher EC. The memory B cell subset responsible for the secretory IgA response and protective humoral immunity to rotavirus expresses the intestinal homing receptor, alpha4beta7. *J Immunol*. 1998;161(8):4227-4235.

29. Biron CA, Cousens LP, Ruzek MC, Su HC, Salazar-Mather TP. Early cytokine responses to viral infections and their roles in shaping endogenous cellular immunity. *Adv Exp Med Biol*. 1998;452:143-149.

30. Steeber DA, Tang ML, Zhang XQ, Muller W, Wagner N, Tedder TF. Efficient lymphocyte migration across high endothelial venules of mouse Peyer's patches requires overlapping expression of L-selectin and beta7 integrin. *J Immunol*. 1998;161(12):6638-6647.

31. Winkelmann R, Sandrock L, Porstner M, et al. B cell homeostasis and plasma cell homing controlled by Kruppel-like factor 2. *Proc Natl Acad Sci U S A*. 2011;108(2):710-715.

32. Hamann A, Andrew DP, Jablonski-Westrich D, Holzmann B, Butcher EC. Role of alpha 4-integrins in lymphocyte homing to mucosal tissues in vivo. *J Immunol*. 1994;152(7):3282-3293.

33. Wagner N, Lohler J, Tedder TF, Rajewsky K, Muller W, Steeber DA. L-selectin and beta7 integrin synergistically mediate lymphocyte migration to mesenteric lymph nodes. *Eur J Immunol*. 1998;28(11):3832-3839.

34. Heidegger S, Kirchner SK, Stephan N, et al. TLR Activation Excludes Circulating Naive CD8+ T Cells from Gut-Associated Lymphoid Organs in Mice. *J Immunol*. 2013;190(10):5313-5320.

35. Pabst O, Herbrand H, Willenzon S, et al. Enhanced FTY720-mediated lymphocyte homing requires G alpha i signaling and depends on beta 2 and beta 7 integrin. *J Immunol*. 2006;176(3):1474-1480.

36. Pabst O, Herbrand H, Willenzon S, et al. Enhanced FTY720-mediated lymphocyte homing requires G alpha i signaling and depends on beta 2 and beta 7 integrin. *Journal of immunology (Baltimore, Md : 1950)*. 2006;176:1474-1480.

37. Mueller SN, Hosiawa-Meagher KA, Konieczny BT, et al. Regulation of homeostatic chemokine expression and cell trafficking during immune responses. *Science*. 2007;317(5838):670-674.

38. Colombi S, Moutschen M, de Leval L, et al. Peyer's patches in murine AIDS: dissociation between lymphoproliferation and anergy. *Scand J Immunol*. 1997;45(2):175-181.

39. Blutt SE, Warfield KL, Lewis DE, Conner ME. Early response to rotavirus infection involves massive B cell activation. *J Immunol*. 2002;168(11):5716-5721.

40. Kuklin NA, Rott L, Feng N, et al. Protective intestinal anti-rotavirus B cell immunity is dependent on alpha 4 beta 7 integrin expression but does not require IgA antibody production. *J Immunol*. 2001;166(3):1894-1902.

41. Teijaro JR, Ng C, Lee AM, et al. Persistent LCMV infection is controlled by blockade of type I interferon signaling. *Science*. 2013;340(6129):207-211.

42. Wilson EB, Yamada DH, Elsaesser H, et al. Blockade of chronic type I interferon signaling to control persistent LCMV infection. *Science*. 2013;340(6129):202-207.

43. Cheng YS, Xu F. Anticancer function of polyinosinic-polycytidylic acid. *Cancer Biol Ther*. 2011;10(12):1219-1223.

44. Manns MP, McHutchison JG, Gordon SC, et al. Peginterferon alfa-2b plus ribavirin compared with interferon alfa-2b plus ribavirin for initial treatment of chronic hepatitis C: a randomised trial. *Lancet*. 2001;358(9286):958-965.

45. Tagliaferri P, Caraglia M, Budillon A, et al. New pharmacokinetic and pharmacodynamic tools for interferon-alpha (IFN-alpha) treatment of human cancer. *Cancer Immunol Immunother*. 2005;54(1):1-10.

FIGURE LEGENDS

Figure 1: Virus-associated immune activation causes rapid disruption of Peyer's patches. (A) Mice were infected with vesicular stomatitis virus (VSV) and 2 or 5 days later, all macroscopically detectable Peyer's patches were isolated. The total cell count for all Peyer's patches per mouse was determined. **(B to D)** Mice were treated twice (day 0 and 3) with poly(I:C) and organs were examined 48 h after the second injection. **(B)** Number of macroscopically detectable Peyer's patches per mouse. **(C)** Mean number of cells in lymphoid compartments per mouse. **(A to C)** Each data point represents one individual mouse and the mean of at least n = 4 mice per group is depicted as a bar. All data are representative of at least two independent experiments. **(D)** H&E-stained paraffin sections of the small intestine from one untreated and one poly(I:C)-treated mouse. The boxes indicate the Peyer's patches depicted below with 40x magnification. These sections are representative of *n* = 3 mice per group. PLN, peripheral lymph nodes. H&E, hematoxylin and eosin

Figure 2: Disruption of Peyer's patches is due to a decrease in B cell numbers. Mice were treated with poly(I:C) as in Fig. 1. Lymphocyte subpopulations were analyzed by flow cytometry. **(A)** Absolute cell numbers and **(B)** poly(I:C)-induced change of lymphocyte subpopulation frequency within all viable cells (difference to untreated in %) in Peyer's patches and PLN were determined. Data indicate the mean value of *n* = 5 mice ± S.E.M and are representative of at least three independent experiments. Treg, regulatory T cells

Figure 3: Disruption of the Peyer's patches is dependent on type I interferons. (A) Mice were treated as in Fig. 1 and organs were examined 48 h after the last poly(I:C) injection. Cell numbers in Peyer's patches and PLN of wild-type and IFNaR-deficient ($IFNaR^{-/-}$) mice are shown. Each data point represents one individual mouse and the mean of *n* = 5 mice per group are depicted as a bar. **(B)** Mice were treated with recombinant IFN-α and organs were examined 24 h after the last injection. Cell numbers in Peyer's patches are shown. Each data point represents one individual mouse and the mean of *n* = 6 mice per group are depicted as a bar. Data are representative of two independent experiments.

Figure 4: Treatment of mice with the $S1P_1$-blocking agent FTY720 counteracts immune-induced disruption of the Peyer's patches. Mice were provided with drinking water supplemented with FTY720 and treated with poly(I:C) as in Fig. 1. Organs were examined 48 h after the last poly(I:C) injection for absolute cell numbers. Data give the mean values of *n* = 10 mice per group ± S.E.M from two independent experiments.

Figure 5: Stimulation with type I interferon results in reduced B cell homing to Peyer's patches. Purified splenic B cells were cultured in the presence of recombinant IFN-α for 24 h. **(A)** Surface expression of CD69, CD62L and $\alpha_4\beta_7$ was determined by flow cytometry. **(B)** Splenic B cells were either stimulated with IFN-α or treated with adhesion molecule-blocking antibodies. Binding of the fluorescently labeled cells to plate-bound MAdCAM-1 was determined by spectrophotometer. All data give the mean value of triplicate samples ± S.E.M. **(C)** IFN-α-stimulated splenic B cells were fluorescently labeled and adoptively transferred into naïve recipient mice. 4 h later, recipients were sacrificed and lymphoid organs assessed for the presence of transferred B cells. The homing index represents the ratio of IFN-α-activated B cells to unstimulated B cells. Data show the mean value of individual recipient mice (*n* = 3) ± S.E.M. The asterisk indicates comparison to the homing index for the spleen. **(D)** Mice were injected i.p. with an anti-$\alpha_4\beta_7$ or an isotype control antibody. 24h later, cell numbers in secondary lymphoid organs were determined by flow cytometry. Data show the mean value of individual mice (*n* = 7 for Peyer's patches and spleen, *n* = 4 for PLN) ± S.E.M pooled from two independent experiments. All data are representative of at least two independent experiments.

Figure 6: Virus-associated innate immune activation does not alter lymphocyte numbers in the intestinal lamina propria. Mice were treated with poly(I:C) as in Figure 1. **(A)** Absolute lymphocyte numbers in the intestinal lamina propria were determined by flow cytometry. Each data point represents one individual mouse and the mean of n = 5 poly(I:C)-stimulated and n = 3 untreated mice per group is depicted as a bar. **(B)** Distribution of $B220^+$ B cells (red) in the intestinal lamina propria was analyzed by immunohistochemistry. **(C)** Serum levels of IgA and IgG were determined by ELISA. Each data point represents one individual mouse and the mean of n = 10 mice per group is depicted as a bar. All data are representative of at least two independent experiments.

Figure 7: Disruption of the Peyer's patches is a self-limiting process. (A) Time course of $\alpha_4\beta_7$ and CD69 expression on circulating B cells in the peripheral blood after a single injection of poly(I:C). Data give the mean value of *n* = 3 individual mice ± S.E.M. The dashed line represents the baseline level of $\alpha_4\beta_7$ expression before treatment. **(B)** Representative histograms are gated on $CD19^+$ blood-borne B cells and give $\alpha_4\beta_7$ and CD69 expression 12 h after poly(I:C) treatment (thin grey line, isotype control). **(C)** Mice were treated with poly(I:C) as in Fig. 1. Time course of total cell numbers in Peyer's patches after the last injection. Each data point represents one individual mouse and the mean of *n* = 5 mice per group is depicted as a bar. All data are representative of at least two independent experiments. Unstim, unstimulated.

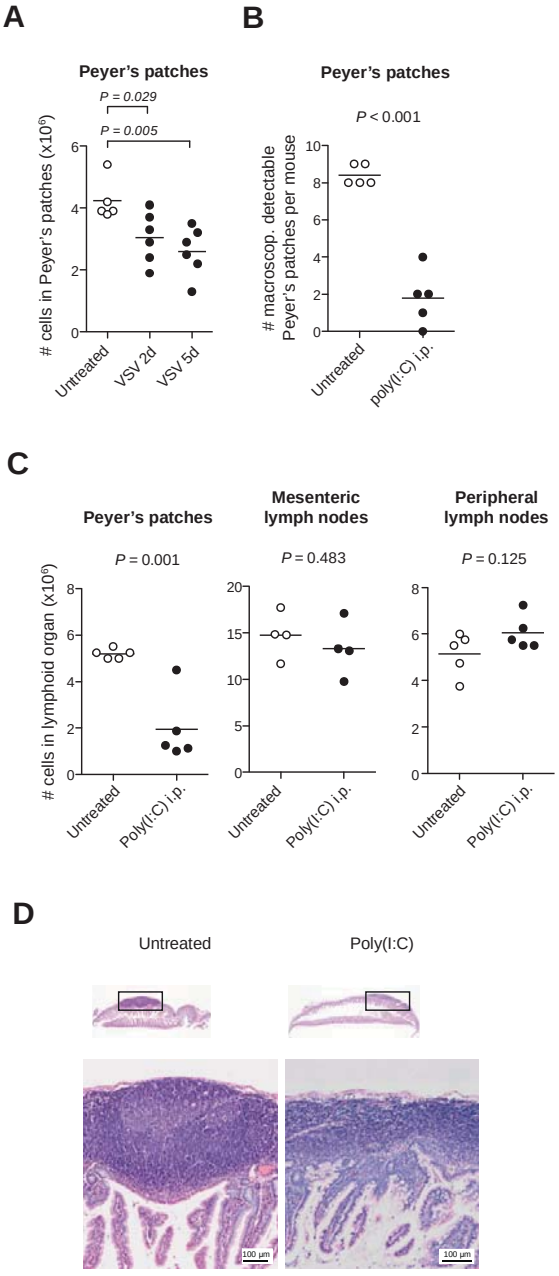

Figure 1

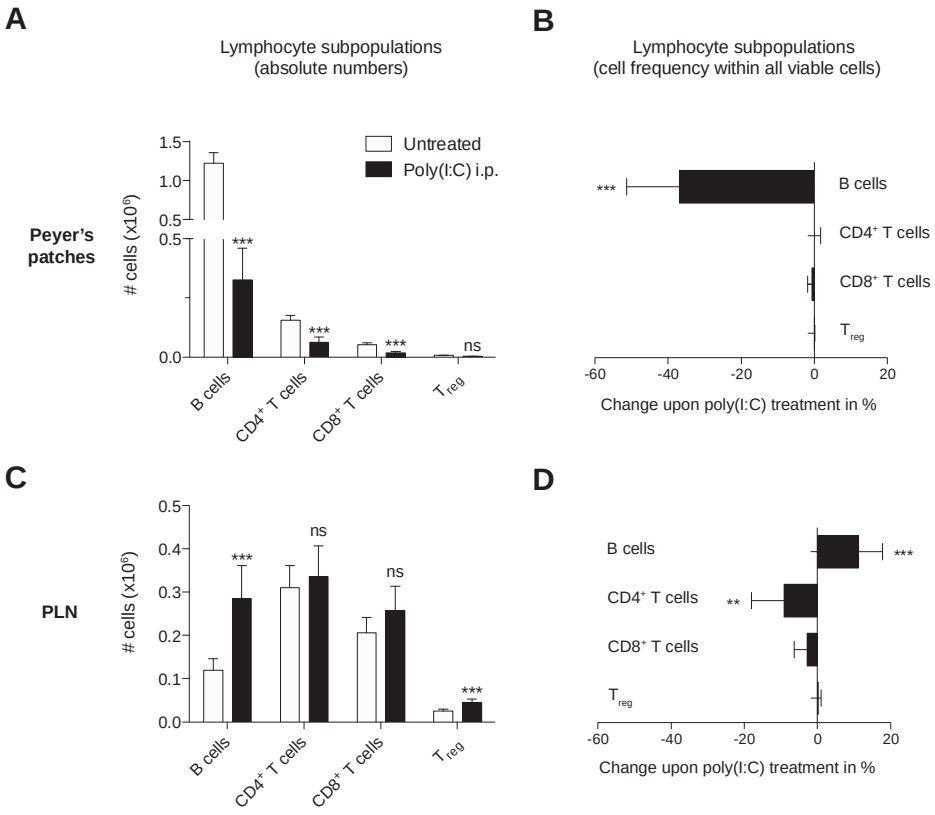

Figure 2

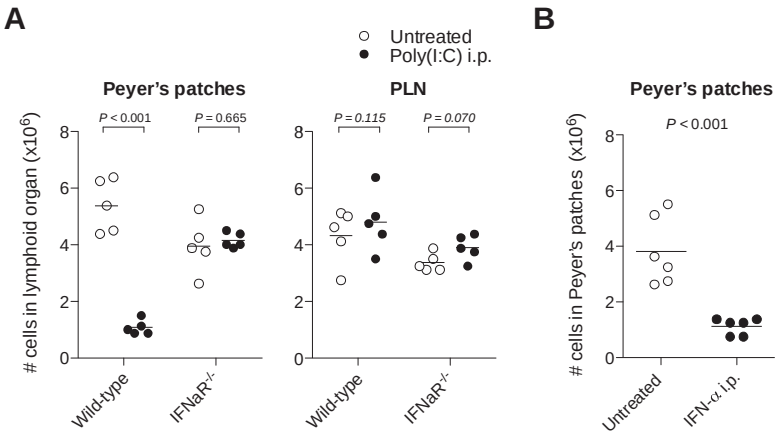

Figure 3

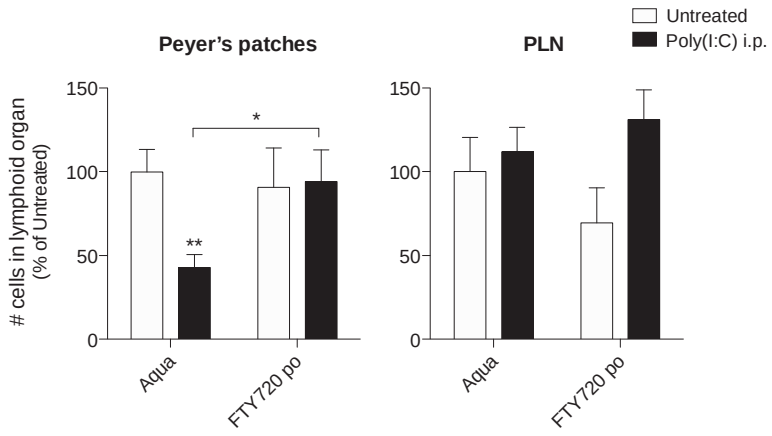

Figure 4

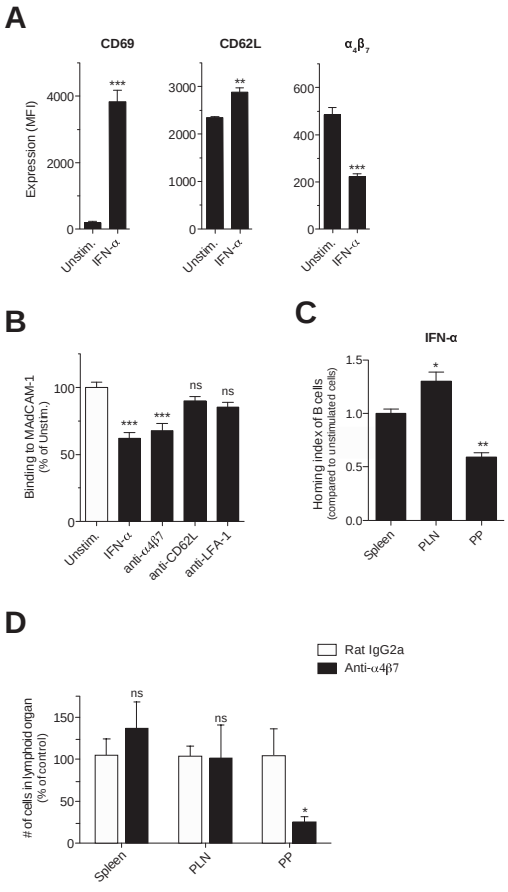

Figure 5

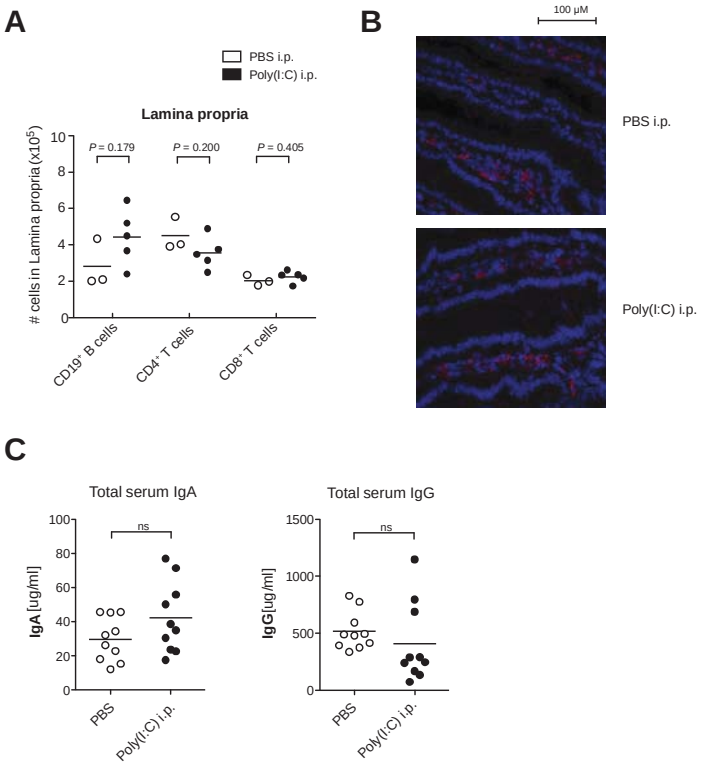

Figure 6

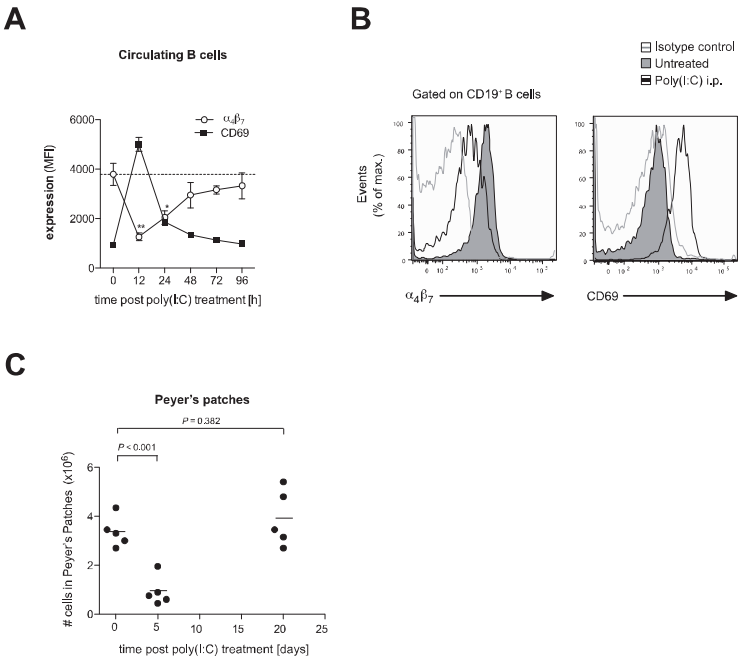

Figure 7